Accepted Manuscript

Hygroscopic strain measurement by fibre Bragg gratings sensors in organic matrix composites – application to monitoring of a composite structure

H. Ramezani-Dana, P. Casari, A. Perronnet, S. Fréour, F. Jacquemin, C. Lupi

PII: S1359-8368(13)00589-1
DOI: http://dx.doi.org/10.1016/j.compositesb.2013.10.014
Reference: JCOMB 2691

To appear in: *Composites: Part B*

Received Date: 25 February 2013
Revised Date: 30 August 2013
Accepted Date: 16 October 2013

Please cite this article as: Ramezani-Dana, H., Casari, P., Perronnet, A., Fréour, S., Jacquemin, F., Lupi, C., Hygroscopic strain measurement by fibre Bragg gratings sensors in organic matrix composites – application to monitoring of a composite structure, *Composites: Part B* (2013), doi: http://dx.doi.org/10.1016/j.compositesb.2013.10.014

Hygroscopic strain measurement by fibre Bragg gratings sensors in organic matrix composites – application to monitoring of a composite structure

*H. Ramezani-Dana, P. Casari, A. Perronnet, S. Fréour, F. Jacquemin, C. Lupi

LUNAM Université - Université de Nantes - Centrale Nantes, Institut de Recherche en Génie Civil et Mécanique (UMR CNRS 6183), 58, rue Michel Ange - BP 420, 44606 Saint-Nazaire, France

E-mail : hossein.ramezani-dana@insa-lyon.fr,

Abstract

This study is devoted to the identification of the moisture expansion coefficients of composite materials by means of a novel measurement technique. This method is based on the insertion of Fiber Bragg Grating (FBG) sensors between composite layers. The sensor enables to measure the hygroscopic strain induced by moisture diffusion in the plane of the laminated composite. Experimental results from immersed samples, varying both the direction of measurement and the fibre volume fraction are given according to the water uptake, and leading to the characterization of moisture expansion coefficient.

Keywords: A. Polymer-matrix composites (PMCs); B. Fiber Bragg grating sensors; C. Environmental degradation

*** Corresponding author:**
hossein.ramezani-dana@insa-lyon.fr, hossein.ramezani_dana@yahoo.com (Tel No: +33612808764)

1. Introduction

Organic matrix composites are extensively used in several engineering applications due to their exceptional stiffness to weight ratio. However, when such materials are exposed to humid environments, they absorb moisture which can severely affect their hygro-mechanical properties [1-3] as well as the multi-scale internal mechanical states experienced by the constituents of polymer matrix composites [4,5]. Consequently, durability and reliability of structural parts made of such materials can be impaired in humid environments. In the glass/polyester composites used in this study, the matrix absorbs a significant amount of water whereas absorption by fibres is almost null. One key issue is to predict the stress state of the material submitted to such environment by means of moisture expansion coefficients. The purpose of this work is exactly to provide such materials parameters and a technique has been developed for it. Numerous authors have used Fibre Bragg Grating (FBG) sensors [6-11] in order to achieve local strain measurements, temperatures and other quantities of engineering interest. An FBG clearly provides many advantages compared to other strain measurement techniques, since it enables to investigate internal mechanical states in the depth of the specimen without suffering from an ageing of the sensor itself.

Then, an experimental study of both the time-dependent moisture uptake and strain field in composite containing FBG sensors has been achieved. Fibre Bragg Grating (FBG) sensors were used to characterize the evolution of hygroscopic strain field in unidirectional fibre-reinforced composite specimens immersed in de-ionized water, during both the transient and the permanent stages of the moisture diffusion process. Besides, the time-dependent average moisture uptake over the volume of the samples was followed through the classical gravimetric method until the permanent regime has been reached. Both longitudinal and transversal moisture expansion coefficients (CME)

of these composite samples were determined by using the data collected through the optical sensors oriented either in a direction parallel or perpendicular to the reinforcing fibres.

2. Materials and testing methods

2.1 Materials and specimens

The tested unidirectional composite samples were made of E-glass fibres embedded in an ortho-phtalic polyester resin (POLYLITE 420-731 from REICHOLD) polymerizing at room temperature. The specimens were manufactured through the vacuum assisted resin infusion (VARI) method.

Several composites, as well as neat resin square plates 1.3 mm thick were fabricated. After cutting and polishing, the samples surfaces were cleaned with ethanol in order to remove any residual oil and dirt resulting from machining. The initial weights and dimensions of the specimens were recorded. The FBGs employed in this study were printed on standard SMF-28e single mode optical fibres with a 250 μm diameter. Bragg gratings (10 mm long) were uniform, and centered on a 1555 ± 0.2 nm wavelength.

The use of FBG in composite samples is limited by the ability to insert this sensor in the composite material in order to retrieve the optical signal without (or the less as possible) modifying the mechanical behaviour of the composite structure considered.

In order to address this issue, the optical fibre containing Bragg grating was inserted between two plates, bonded by polyester resin. The FBG were either aligned with the reinforcing fibres or set perpendicularly to them.

In the area of the grating, the FBGs acrylate coating was removed in order to get the most direct strain provided by the surrounding material towards the sensor.

This type of specimen architecture enabled us to obtain instrumented samples, the final size of which is 90x90x3 mm^3. In addition, this kind of architecture allows us to limit the stresses experienced by optical fibre during the fabrication process.

The main parameters controlling moisture diffusion kinetics, namely the diffusion coefficients and the maximum moisture absorption capacity, do strongly depend on the volume fraction of the constituents (i.e., those of the reinforcing fibres and the polymeric matrix). Therefore, the reinforcing fibres content of the composite affects the magnitude of the multi-scale mechanical states to be monitored during the present work. As a consequence, the accurate characterization of the volume fraction occupied by glass fibres in each investigated sample was mandatory in the context of the present work. Several techniques have historically been employed in order to determine the fibre volume fraction (v_f) of organic matrix composites [12-14]. In the present work, the identification of the glass-fibre volume fraction in the manufactured samples will be handled according to a dimension and weight analysis method.

Optical microscopy and Scanning Electron Microscopy were used for investigating the microstructure of the manufactured samples (see figure 1). According to both characterization methods, specimens are void-free.

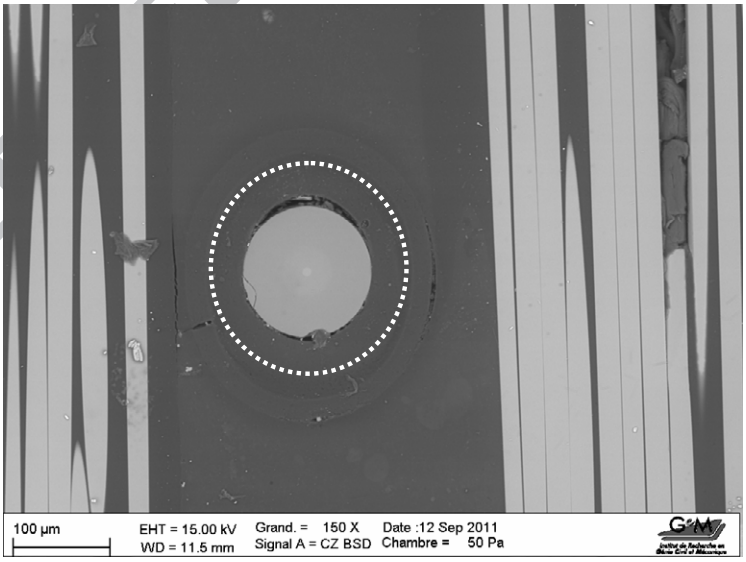

Figure 1 . SEM micrograph showing an optical fibre embedded perpendicularly to the reinforcing fibres (white dashed line circle illustrates the optic fibre coating).

As a result, the total volume of the composite (V_t) is equal to the sum of the volume occupied by the glass fibres (V_f), on the one hand and by the resin (V_r), on the other hand:

$$V_t = V_f + V_r \quad (1)$$

A similar relation is also valid for the corresponding masses:

$$m_t = m_f + m_r = \rho_f V_f + \rho_r V_r = \rho_t V_t \quad (2)$$

where ρ denotes the mass density. The total density respects the following classical mixture law:

$$\rho_t = \rho_t v_f + \rho_r v_r = \rho_f v_f + \rho_r (1 - v_f) \quad (3)$$

The reinforcing fibres volume fraction corresponds to the following ratio:

$$v_f = \frac{V_f}{V_t} = \frac{1}{\rho_f - \rho_r}\left[\frac{m_t}{V_t} - \rho_r\right] = \frac{\rho_t - \rho_r}{\rho_f - \rho_r} \quad (4)$$

Dimensions and mass of the specimens were measured in order to determine their total volume (V_t) and their total mass (m_t), from which the total mass density calculation is straightforward. The same method was applied to the neat resin samples, so that the numerical

value of ρ_r could be deduced. Glass fibres mass density is a well known parameter that is widely available in the literature [15]. The results obtained through this calculation method, for the glass fibres volume fraction, are displayed in table 1.

Specimen group N°	1	2	3
v_f (%)	17	21	22

Table 1. Fibre volume content of the manufactured samples.

2.2 Experimental set up and hygroscopic ageing process

Two series of specimens were manufactured. The first subset of samples was instrumented by FBGs sensors. FBGs were oriented perpendicular or parallel to the

reinforcing fibres. This group of samples was intended to provide the time-dependent evolution of the internal strains states throughout the moisture diffusion process. The second subset of specimens, which did not contain any optical fibre, was devoted to moisture uptake characterization by means of periodic mass measurements. The samples were also immersed in de-ionized water.

The optical measurement system used is constituted as follows: The optical source is a broadband optical source in C-Band (1530-1560 nm) based on erbium doped Amplified Spontaneous Emission. This light source is connected to a 2-1 optical coupler. The optical output coupler is connected to a FBGs realized in a standard SMF-28e single mode optical fiber. The Bragg grating length is 10 mm. The reflected signal is received through the optical coupler by an Optical Spectrum Analyzer (Anritsu MS9710B) with 70 pm wavelength resolution. The spectral signature of the Bragg grating is numerically analyzed in order to determine the measured strain during the hygroscopic ageing test imposed to the samples.

2.3 Technique of measurement

Mechanical strains measurements through FBG have been presented in various papers [16, 17]. A FBG consists in a series of grating slices formed along the fibre axis. If the Bragg condition is fulfilled, a light signal propagating into the device can interfere constructively to the waves reflected by each of the slices. As a result, a back reflected signal with a center wavelength commonly known as the Bragg wavelength λ_b is formed. Bragg-wavelength λ_b depends on the effective index of refraction (n_{eff}) and on the Bragg period (Λ) of the grating according to the well known Bragg equation (eq. 5).

By inscribing several FBGs with different grating periods in the same optical fiber, an array of grating is manufactured. This allows the user to monitor different positions in the structure with only one sensor line [18].

$$\lambda_b = 2n_{eff}\Lambda \qquad (5)$$

In the case when the FBG is submitted to a homogeneous axial strain ε_z and uniform temperature change ΔT, the Bragg wavelength experiences a deviation $\Delta\lambda_b$ from the reference value λ_{b0} corresponding to the unloaded state ($\varepsilon_z = 0$; $\Delta T = 0$):

$$\frac{\Delta\lambda_b}{\lambda_b} = \frac{\lambda_b - \lambda_{b0}}{\lambda_b} = a\varepsilon_z + b\,\Delta T \qquad (6)$$

Coefficients a and b depend on the nature of the optical fibre and the FBG printing parameters. According to relation (6), under isothermal conditions, the Bragg wavelength shift $\Delta\lambda_b$ is proportional to the axial strain (ε_z).

According to expression (6), one obvious major limitation of FBG sensors in composites is the sensitivity to both the deformation and the temperature. As a result to measure moisture absorption through the deformation variation, the temperature must be simultaneously measured to determined thermo-optic effect and thermo-mechanical deformations to determine deformations only due do moisture absorption.

In the present study, the strong hygroscopic strain experienced by organic matrix composites exposed to moisture diffusion is expected to induce an axial elongation of the optic fibre containing the Bragg grating [19], resulting in a significant Bragg wavelength shift according to equation (6).

3. Results and discussion

3.1 Hygroscopic aging tests

The curves of weight gain versus the square root of time obtained for the neat resin as well as those corresponding to the composite samples are shown on figure 2a and 2b, respectively.

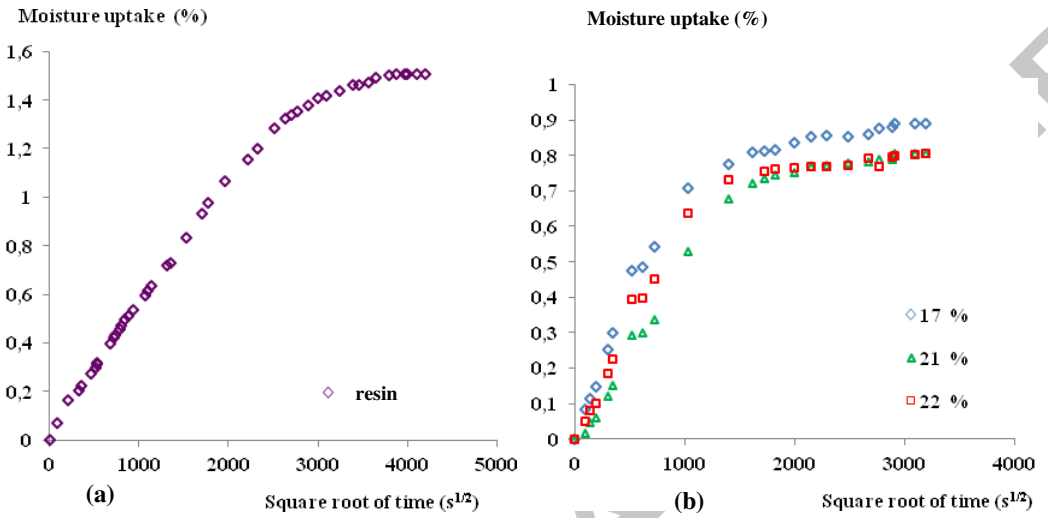

Figure 2. The weight gain versus the square root of time ($\sqrt{t}$) curves for resin specimen (a) and composite specimens with different fibre content (b).

The neat resin (figure 2a) exhibits a time-dependent moisture uptake typical from Fickian kinetics. According to figure 2b, the three composite samples exhibit an almost linear evolution of their moisture uptake for several months until a pseudo-plateau indicating that the saturation of the diffusion process is reached. Thus, it is realistic to also consider a fickian diffusion behavior for the investigated composite samples.

The identification method of the diffusion parameters used in this study was explained in [20]. This method was consisting in identifying the unknowns of the problem by minimizing the standard deviation between the calculated and measured quantities using a Gauss-Newton algorithm.

The moisture diffusion parameters of both composite and neat resin specimen are then presented in table 2:

	$D_{apparent}$ (mm^2/s)	D_2 (mm^2/s)	**Ms** (%)
Composite (v_f = 17 %)	$2.2*10^{-7}$	$2.07*10^{-7}$	0.85
Composite (v_f = 21 %)	$2.1*10^{-7}$	$1.74*10^{-7}$	0.78
Composite (v_f = 22 %)	$1.83*10^{-7}$	$1.97*10^{-7}$	0.79
Bulk resin	$2.31*10^{-7}$	$2.31*10^{-7}$	1.5

Table 2. Moisture diffusion parameters of composite and neat resin.

3.2 Internal strain measurement

The measured Bragg's wavelength shift enables to determine strain experienced in the center of the instrumented samples, from relation 6, assuming that the thermal contribution, namely, the product $b\,\Delta T$ is negligible by comparison to the quantity of interest: $a.\varepsilon_z$.

Figure 3 shows the evolution as a function of the square root of time of the hygroscopic strain, obtained for the three composite specimens instrumented by FBG positioned perpendiculary to the reinforcing fibres. Room temperature change of the ambient fluid monitored during the ageing test is also displayed on the same figures. One can observe three steps on this figure. We can note a very light induced strain during first day for the samples containing 17 % and 22 % of glass fibres in opposite to the sample with 21 % of glass fibres. Indeed this sample (v_f=21%) was released in order to characterize the Bragg grating properties before water ageing effects. This specimen sinks in again after some days. This last, led to the ageing period shifting for this specimen. In the second step, we can note a quasi linear behavior of deformation during several months. Finally, the last step corresponds to the permanent regime of the diffusion process. A significant scattering of the hygroscopic strains can be noticed during last step. This scattering almost follows the temperature change of the ambient fluid, which ranges from 25°C to 31°C throughout the ageing test.

Such a temperature change strongly affects the Bragg wavelength and consequently the measured strain.

As an example, we found the hygroscopic strain close to $4600*10^{-6}$ at 31°C for the sample containing 17 % of fibres. This value decreased to $3800*10^{-6}$ at 25°C. This variation of the strain in the saturation state could be explained by a temperature change. Figure 3b shows the evolution of the strain as a function of square root of time for the three composite specimens instrumented by FBG positioned in a direction parallel to the reinforcing fibres. The measured strain in this direction is smaller in comparison to the first case (a). In fact, in the direction parallel to the reinforcements (b), the moisture expansion coefficient of unidirectional composite is usually lower than in the direction perpendicular to the reinforcements (a), which induces smaller hygroscopic strain during the moisture diffusion process.

The effect of temperature variations on the measured strain is also significant; therefore, the determination of purely hygroscopic strain value is not easy, particularly in a direction parallel to the reinforcing fibres.

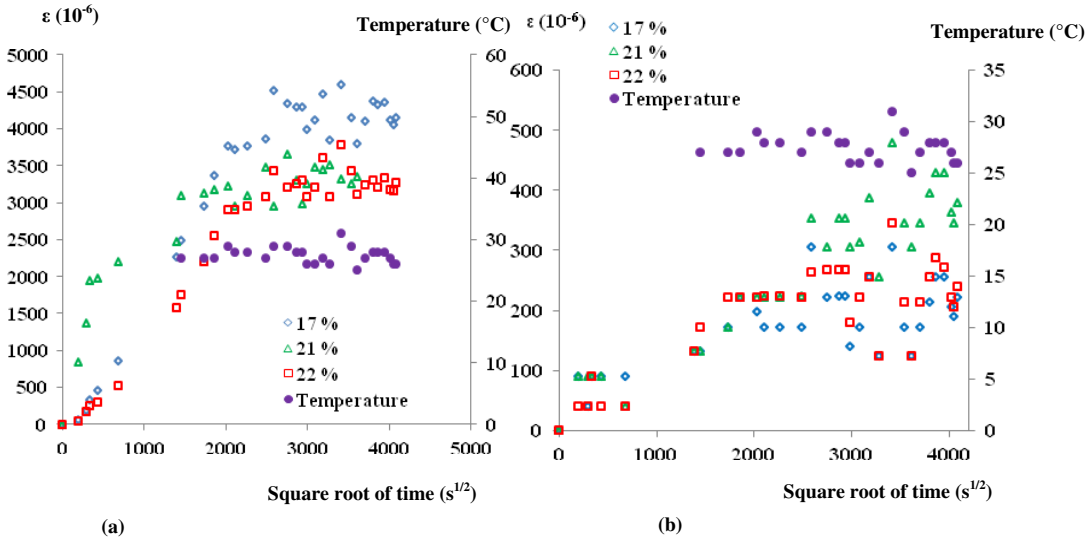

Figure 3. Evolutions of the strain as a function of square root of time for the composite specimens instrumented perpendicularly (a) and parallely (b) to the reinforcing fibres.

Figure 4a shows the evolution, as a function of moisture uptake, of the hygroscopic strain obtained for the three composite specimens instrumented by FBG oriented in a direction perpendicular to the reinforcing fibres. Such a curve has to be analyzed in order to deduce the coefficient of moisture expansion of the studied specimens.

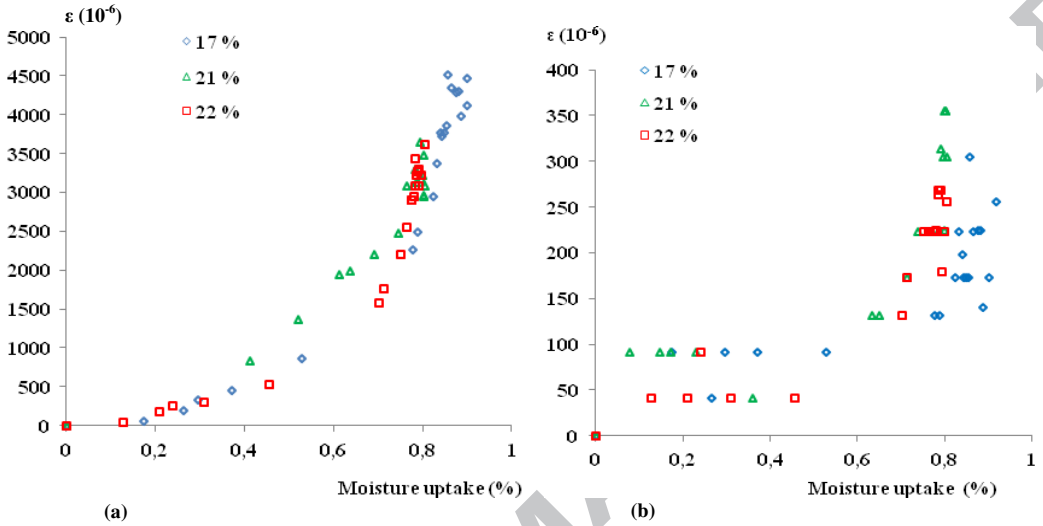

Figure 4. Strain as a function of moisture uptake for composite specimens instrumented perpendicularly (a) and parallel (b) to the unidirectional fibres.

According to figure 4, the measured strain remains close to zero at the beginning of ageing process. A quasi-linear evolution of strain up to a sample saturation state was found. One can observe that strains keep on increasing while the specimen has reached saturation. This is explained because the measured moisture uptake is an average value from the whole sample volume, whereas strains are measured in the center of composite specimen where FBGs were located. The strain value of specimen with 17 % glass fibre content is higher in this direction, which is due to a higher resin volume fraction.

When FBGs are oriented parallel to the reinforcing fibres (b), hygroscopic strains vary much less and exhibit a significant scatter. As temperature variations contribute to the Bragg peak shift, it is necessary to correct this effect before analyzing more accurately figures 4a and 4b.

The Bragg wavelengths from before and after ageing and the corresponding strains were gathered in table 3.

$\mathbf{v_f}$ (%)	**A**ngle (°)	λ_b (nm) Before immersion	λ_b (nm) After immersion	$\Delta\lambda_b$ (nm)	ε (10^{-6})
17	0	1554.68	1554.95	0.27	255
17	90	1550.98	1556.01	5.03	4157
21	0	1554.68	1555.14	0.46	379
21	90	1551.48	1555.93	4.45	3677
22	0	1554.68	1554.97	0.29	239
22	90	1550.81	1555.18	4.37	3611

Table 3. Hygroscopic strain for all instrumented specimens

3.3 Correction from thermal expansion

A part of the strain scatter in the Bragg peak shifts is the effect of temperature leading to both a variation of the optical index associated to a global thermal expansion of both the composite laminate and the optical fibre. In order to determine a better estimate of hygroscopic strains, temperature effects are corrected.

Several methods have been proposed in the literature to achieve this task, as an example by combining multiple sensors or by using a specific sensor [21-28]. In this study, we propose a quick but reliable method. Actually, additional information is necessary. For this purpose, a thermal loading has been conducted once the laminates reached a saturated state. The result on strain is plotted in figure 5 for the three composite specimens instrumented by FBG positioned perpendicularly (figure 5a) or parallel (figure 5b) to the reinforcing fibres, respectively.

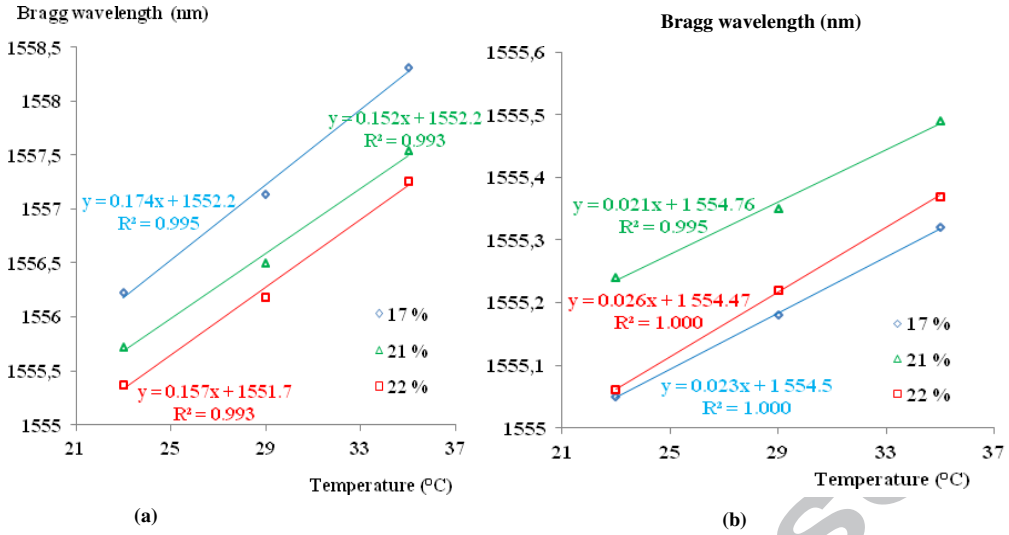

Figure 5. Bragg wavelength as a function of temperature for the composite specimens instrumented perpendicularly (a) and parallel (b) to the reinforcing fibres.

From the slope of the curves presented on figures 5a and 5b, one can separate the effects induced by the temperature change from that of the hygroscopic strain on the measured Bragg wavelength shifting λ_b. A linear change of the Bragg wavelength occurs as a function of temperature from 23°C to 35°C in the studied directions. The composites specimens, in which FBG sensors were positioned in a direction perpendicular to the reinforcing fibres (figure 5a) show greater slope of Bragg shifting in comparison to the specimens, in which FBG sensors were oriented parallel to the reinforcing fibres (figure 5b). These results are used to correct the measured strain from a known temperature shift. Indeed by using the graph trend slope of these curves ($\lambda = f(T)$), sensitivity of Bragg wavelength to the temperature was deduced. Accordingly, the contribution due to the temperature on the Bragg peak shifts could be determined and separated from the total strain, so that the neat hygroscopic strain was eventually estimated through (7).

$$\varepsilon_{hyg} = \varepsilon_{tot} - \varepsilon_{ther} \qquad (7)$$

According to the measurements, the sensitivity is higher in the direction perpendicular to the reinforcing fibres.

Figure 6a represents strains before and after correction as a function of the square root of time for the composites specimen with 17 % fibre contents instrumented by FBG oriented in a direction perpendicular to the reinforcing fibres. The saturation pattern of strains curve for this sample is better defined in comparison to the uncorrected measurements. In contrary, the deformation of the composite specimen with 17 % fibre content instrumented by FBG positioned parallel to the reinforcing fibres (figure 6b) remains scattered after correction of the effect of temperature. This last could be explained by local heterogeneities of the lamination. Globally, measured strains decrease by removing the effect of temperature from the strain response to moisture.

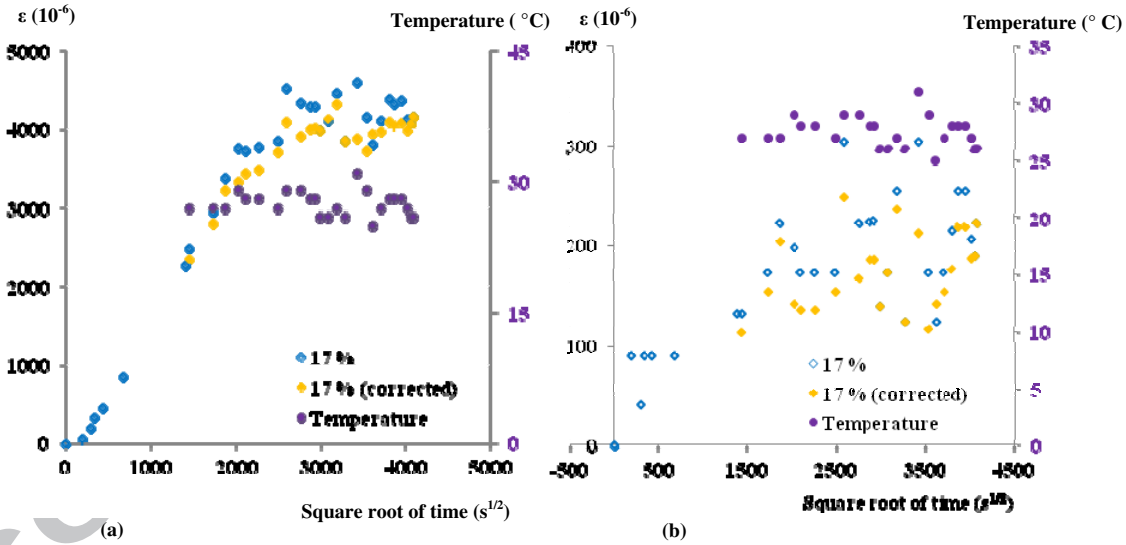

Figure 6. Strains evolution as a function of square root of time for the composite specimens instrumented perpendicularly (a) and parallel (b) to the reinforcing fibres.

Figure 7 shows the corrected strains as a function of moisture content for the three composite specimens instrumented by FBG positioned either in a direction perpendicular (figure 7a) or parallel (figure 7b) to the reinforcing fibres, respectively.

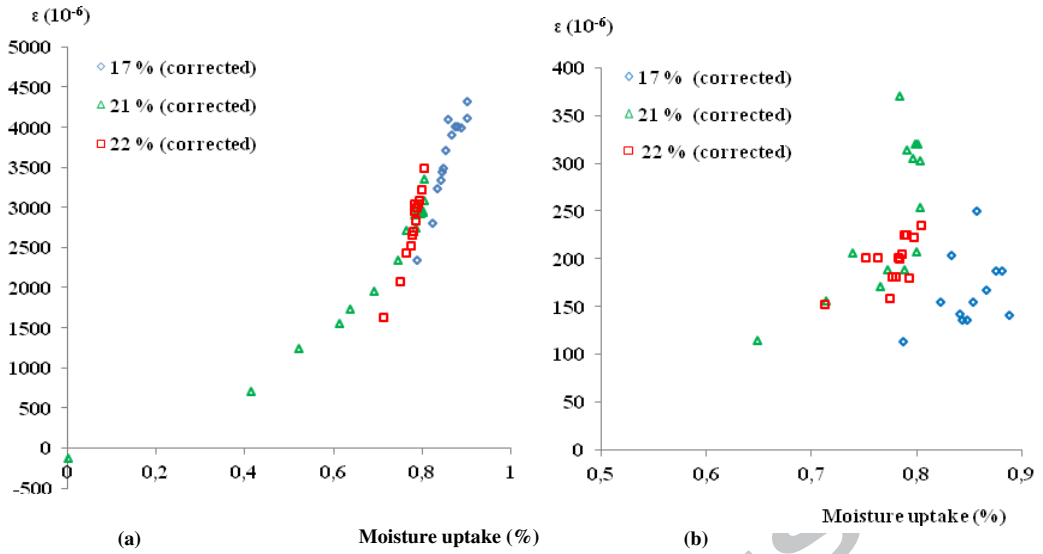

Figure 7. Evolutions of the strain as a function of moisture content for the composite specimens instrumented perpendicularly (a) and parallel (b) to the reinforcing fibres.

According to figure 7a, the evolution of hygroscopic strain and the saturation pattern of the three samples are better defined in comparison to non corrected state. Unfortunately, at this step, we can see also a bit of disturbance on the saturation pattern for the specimen with 17 % fibre content. Knowing that this disturbance appears in a saturated state, consecutive evolution of the deformation is probably associated to a defect of the microstructure, such as a cracking. Hygroscopic strain in the direction parallel to the reinforcements (figure 7b) is hard to explain, due to the very small strains experienced by the three composite specimens in that direction.

From the curves of the hygroscopic strain as a function of the water uptake, one can also determine the coefficients of moisture expansion of the studied samples. The moisture expansion coefficients are determined by considering the strains and moisture contents in the steady state:

$$\beta_{11} = \frac{\varepsilon_{11}}{M_S} \quad (8)$$

$$\beta_{22} = \frac{\varepsilon_{22}}{M_S} \quad (9)$$

The values of these coefficients are given in table 4:

$\mathbf{v_f}$ (%)	$\mathbf{M_s}$ (%)	ε_{11} (10^{-6})	ε_{22} (10^{-6})	β_{11}	β_{22}
17	0.85	180	4000	0.021	0.471
21	0.79	330	3140	0.042	0.397
22	0.78	200	3100	0.026	0.397

Table 4. Mechanical and hygroscopical properties of elaborated samples.

4. Conclusions

In this work, the hygroscopic strains experienced by composite samples immersed in de-ionized water were followed from the transient to the permanent stage of the diffusion process. The measurements were carried out owing to Fibre Bragg Grating (FBG) sensors. The results obtained by this method confirm the pertinence of FBG sensors to measure the local strain.

In this study, the thermal strains due to the temperature change during the experimental investigation have been determined in order to identify a more realistic estimation of the hygroscopic strains.

The hygroscopic strain has been identified in a direction parallely and perpendicularly to the reinforcing fibres. The combination of the obtained results to the knowledge of the moisture uptake enables the identification of the macroscopic coefficients of moisture expansion of the studied samples, also.

References

[1] Shen CH, Springer GS. Moisture absorption and desorption of composite materials. Journal of Composite Materials 1976; 10:2-20.

[2] Weitsman YJ. Fatigue of composite materials. New York: Elsevier, 1991.

[3] Selzer R, Friedrich K. Mechanical properties and failure behavior of carbon fibers-reinforced polymer composites under the influence of moisture. Composite Part A 1976; 28:595-604.

[4] Youssef G, Fréour S, Jacquemin F. Stress-dependent Moisture Diffusion in Composite Materials. Journal of Composite Materials 2011; 43:1621-1637.

[5] Sar BE, Fréour S, Davies P, Jacquemin F. Coupling Moisture Diffusion and Internal Mechanical States in Polymers - A Thermodynamical Approach. European Journal of Mechanics 2012; 36:38-43.

[6] Karalekas D, Cugnoni J, Botsis J. Monitoring of hygrothermal ageing effects in an epoxy resin using FBG sensor: A methodological study. Composites Science and Technology 2009; 69:507-514

[7] Pereira G, Frias C, Faria H, Frazão O, Marques AT. On the improvement of strain measurements with FBG sensors embedded in unidirectional composites. Polymer Testing 2013; 32:99–105.

[8] Mihailov SJ. Fiber Bragg Grating Sensors for Harsh Environments. Sensors 2012; 12(2): 1898-1918.

[9] Frieden J, Cugnoni J, Botsis J, Gmür T, Ćorić D. High-speed internal strain measurements in composite structures under dynamic load using embedded FBG sensors. Composite Structures 2010; 92:1905–1912.

[10] Mulle M, Collombet F, Olivier P, Zitoune R, Huchette C, Laurin F, Grunevald YH. Assessment of cure-residual strains through the thickness of carbon–epoxy laminates using FBGs Part II: Technological specimen. Composites Part A: Applied science and Manufacturing 2009; 40(10):1534–1544.

[11] Yeo TL, Sun T, Grattan KTV. Fibre-optic sensor technologies for humidity and moisture measurement, Sensors and Actuators A 2008; 144:280-295

[12] Ye BS, Svenson AL, Bank LC. Mass and volume fraction properties of pultruded glass fibre-reinforced composites. Composites 1995; 26(10):725-731.

[13] Green P, Fibre volume fraction determination of carbon-epoxy composites using an acid digestion bomb. Journal of Materials Science Letters 1991; 10(19):1162-1164.

[14] Ye BS, Svenson AL, Bank LC. Mass and volume fraction properties of pultruded glass fibre-reinforced composites. Composites 1995; 26(10):725-731.

[15] Herakovitch CT. Mechanics of Fibrous Composites. New York: John Wiley and Sons Inc., 1998.

[16] Helan R, Urban F. Principle of Fiber Bragg Gratings Measurement. In Proceeding of *30th* International Spring Seminar on Electronics technology (ISSE/30). Cluj Napoca, Romania, 2007.

[17] Giaccari P, Dunkel GR, Humbert L, Botsis J, Limberger HG, Salathé RP. On a direct determination of non-uniform internal strain fields using fibre Bragg grating. Smart Materials and structures 2005; 14(1):127-136.

[18] Luyckx G, Voet E, Lammens N, and Degrieck Y. Strain Measurements of Composite Laminates with embedded Fibre Bragg Gratings: Criticism and Opportunities for Research. Sensors 2011; 11(1):384-408.

[19] Frieden J, Cugnoni J, Botsis J, Gmür T. High-speed internal strain measurements in composite structures under dynamic load using embedded FBG sensors. Composite Structures 2010; 92:1905–1912.

[20] Ramezani dana H, Perronnet A, Freour S, Casari P and Jacquemin F. Identification of moisture diffusion parameters in organic matrix composites. Journal of Composite Materials 2013; 47(9):1081-1092.

[21] Li T, Dong X, Chan CC, Hu L, Qianà W. Simultaneous strain and temperature measurement based on a photonic crystal fiber modal-interference interacting with a long period fiber grating. Optics Communications 2012; 285:4874-4877.

[22] Xia L, Shuai B, Li W, Liu D. Simultaneous measurement of temperature and infinitesimal displacement using the high cladding mode coupling loss in fiber Bragg grating. Sensors and Actuators A 2012; 176:53-56.

[23] Valdivielso F, Matías IR, Arregui FJ. Simultaneous measurement of strain and temperature using a fiber Bragg grating and a thermochromic material. Sensors and Actuators A 2002; 101:107-116.

[24] Cavaleiro PM, Araújo FM, Ferreira LA, Santos JL, Farahi F. Simultaneous measurement of strain and temperature using Bragg gratings written in germanosilicate and boron-codoped germanosilicate fibers. IEEE Photonics Technology Letters 1999; 11(12):1635-1637.

[25] Enríquez DA, Cruz ARD, Thereza M, Giraldi MR. Hybrid FBG–LPG sensor for surrounding refractive index and temperature simultaneous discrimination. Optics & Laser Technology 2012; 44(4):981-986.

[26] Kang HK, Ryu CY, Hong CS, Kim CG. Simultaneous Measurement of Strain and Temperature of Structures Using Fiber Optic Sensor. Journal of Intelligent Material Systems and Structures 2001; 12(4):277-281.

[27] Rao YJ, Yuan SF, Zeng XK, Lian DK, Zhu Y, Wang YP, Huang SL, Liu TY, Fernando GF, Zhang L, Bennion I. Simultaneous strain and temperature measurement of advanced 3-D Braided composite materials using an improved EFPI/FBG system. Optics and lasers in Engineering 2002; 38(6):557-566.

[28] Lopez-Higuera JM, Echevarria J, Quintela A, Jauregui C, Cobo A, Strain and temperature transducer on one fiber Bragg grating. In proceedings of 8th Annual International Symposium on Smart Structures and materials (SPIE/8), Newport Beach, California, USA, March, 2001.p.192-198.